Bearing / Contact for Anisotropic Materials

Tseng-Hua Tsiang* and John F. Mandell†
Massachusetts Institute of Technology, Cambridge, Massachusetts

The bearing/contact behavior of fiber composites has been investigated using a modified nonlinear assumed stress hybrid finite element formulation. The problem considered is an anisotropic body subjected to compressive contact from an isotropic indentor, with moderate sliding on the contact surface. The characteristic matrices of the bodies brought into contact are obtained by employing a modified principle of the minimum complementary energy, and using the contact conditions along the contacting boundary as constraints with corresponding Lagrangian multipliers. A computer program has been developed for the two-dimensional punch problem. The stick-slide behavior and frictional effects are performed using an iterative technique. Thirty cases of the punch/contact problem have been analyzed. Results for typical variations in properties show that, for the same frictional condition, the material stiffness in the indentation direction dominates the stresses on the contacting surface. By increasing the friction on the contact surface, the transverse tensile stress is relaxed; this can be directly related to suppression of fiber-resin debonding or splitting in practical bearing problems.

Introduction

THERE is widespread interest in the effects of structural connections on the performance of fiber composites. Due to their anisotropy, the structural behavior of composites is different for conventional isotropic materials. As a bearing load is transferred from one member to another at a connection, bearing/contact stresses are generated over the limited area of contact. Although most design of structural members is associated with stresses and strains in portions of the body far from the points of application of loads, the stresses on or somewhat beneath the surface of contact may still be the major cause of failure of one or both of the bodies. The size and shape of the contact area and the frictional conditions on the contact surfaces are important factors in the study of load-bearing/contact problems.

The stress and deformation fields developed during the contact of two mechanically joined parts are important aspects in damage initiation. Between the two surfaces that are pressed together, the principal compressive stress is maximum on the contact surface, whereas the maximum shear stress occurs slightly below the contact area, as shown analytically by early researchers.[1-3] In analysis of the distortion of two elastic bodies progressively pressed together, it is necessary to consider the nonlinearity introduced by the increasing area of contact and frictional stick-slide behavior on the contact plane. Analytical solutions limited to simple geometries and ideal loading conditions are not adaptable to these conditions.

Problems concerned with indentation have been investigated for many years. Indentation is defined as a particular contact problem because the contact area remains constant. Early in 1952, Okubo[1] gave a mathematical solution for a plane-strain flat punch into a semi-infinite elastic body. The pressure distribution between two elastic bodies pressed together was presented. The material properties of the two contact bodies were found to significantly affect the contact situation and the pressure distribution. However, a more general numerical approach for solving this nonlinear problem is needed. In recent years, attempts have been made using finite element techniques and complex iterative contact procedures. Yamada et al.,[4] Ohte,[5] Tsuta and Yamaji,[6] and Boonluator[7] applied conventional assumed displacement finite element models. Kubomura and Pian[8] investigated the extensive sliding contact problem by using the assumed stress hybrid finite element model, regarding the contact conditions as constraints in the modified complementary energy principle.

In the present work, the punch/contact problem is treated as elastic bodies with moderate sliding on the contact surface. The characteristic matrices of the bodies brought into contact are obtained by using a finite element discretization with two-dimensional assumed stress hybrid elements. Moderate sliding is defined by small relative sliding between a contact node pair compared with the element size. Based upon the work of Kubomura and Pian, a modified finite element formulation is carried out. For a practical metal-composite bearing case, the punch is modeled as isotropic and the semi-infinite body as anisotropic.

Contact Stress Analysis

Generally, no prescribed conditions can be set in the case of elastic-body contact, since not only does the contacting surface change at each load step, but the relative motion between the node pair at the edge of the contact changes. Therefore, one has to search the candidate node pairs of contact at every load step and determine their positions with respect to the contacting surface—in separation, in penetration, or in contact—by using the convergent criteria of incremental nodal displacements. In addition, Coulomb's frictional law at the contacting surface must be satisfied,

$$R_s + \mu R_n = 0 \tag{1}$$

where R_n and R_s are the normal and tangential forces on the contact surface. It is noted that the sign of the coefficient of friction μ depends on the direction of displacement of a point on the surface of the elastic body relative to the indentor.

For the continuity conditions between contact surfaces, the criteria are:

1) The displacements normal to the contact surface are common to both bodies.

$$U_n^A = U_n^B \tag{2}$$

2) The tractions over the contact area are also common but in opposite directions.

$$T_n^A + T_n^B = 0, \qquad T_s^A + T_s^B = 0 \tag{3}$$

Received June 18, 1984; revision submitted Sept. 14, 1984.

*Currently, Senior Research Engineer, Advanced Composites R&D, Rohr Industries, Inc., Chula Vista, Calif. Member AIAA.

†Principal Research Associate, Department of Materials Science and Engineering.

However, in the case of frictional sliding, the tangential components of tractions must be determined by the normal components of tractions using Coulomb's law,

$$|T_s| < |\mu T_n| \tag{4}$$

If $|T_s| > |\mu T_n|$, the traction relationship should be given as

$$|T_s| = |\mu T_n| \tag{5}$$

If there is no sliding, the tangential displacements on the contact surfaces are common,

$$U_s^A = U_s^B \tag{6}$$

A modified principle of the minimum complementary energy is employed in the present analysis. The contact conditions along the contacting boundary are considered constraints with corresponding Lagrangian multipliers. The finite element formulation for the punch problem can be expressed as

$$\pi_{mc}^P = \sum_n \left\{ \frac{1}{2}\int_{V_n} \boldsymbol{\sigma}^T \boldsymbol{C}\boldsymbol{\sigma}\,\mathrm{d}v - \int_{\partial V_n} \boldsymbol{T}^T \tilde{\boldsymbol{u}}\,\mathrm{d}s + \int_{s_{\sigma_n}} \bar{\boldsymbol{T}}^T \tilde{\boldsymbol{u}}\,\mathrm{d}s - \int_{s_{c_n}} \tilde{\boldsymbol{T}}^T [\boldsymbol{u}^A - \boldsymbol{u}^B]\,\mathrm{d}s \right\} \tag{7}$$

where stresses, $\boldsymbol{\sigma} = \boldsymbol{P}\boldsymbol{\beta}$; boundary displacements, $\boldsymbol{u} = \boldsymbol{L}\boldsymbol{q}$; surface tractions, $\boldsymbol{T} = \boldsymbol{R}\boldsymbol{\beta}$; tractions on contact boundary, $\tilde{\boldsymbol{T}} = \boldsymbol{M}\boldsymbol{t}$; and boundary displacements on the contact boundary in bodies A and B are, respectively,

$$\boldsymbol{u}^A = \boldsymbol{L}^A \boldsymbol{q}^A, \qquad \boldsymbol{u}^B = \boldsymbol{L}^B \boldsymbol{q}^B \tag{8}$$

where s_{c_n} is the contacting boundary of the nth element and $\boldsymbol{t}$ the element nodal traction on the contacting boundary.

The functional for the nth element can be written as

$$\pi_{mc_n}^P = \tfrac{1}{2}\boldsymbol{\beta}^T \boldsymbol{H}_n \boldsymbol{\beta} - \boldsymbol{\beta}^T \boldsymbol{G}_n \boldsymbol{q}_n + \boldsymbol{Q}_n^T \boldsymbol{q}_n - \boldsymbol{t}^T\left(\boldsymbol{F}_n^A \boldsymbol{q}_n^A - \boldsymbol{F}_n^B \boldsymbol{q}_n^B\right) \tag{9}$$

where

$$\boldsymbol{H}_n = \int_{V_n} \boldsymbol{P}^T \boldsymbol{C}\boldsymbol{P}\,\mathrm{d}v \tag{10}$$

$$\boldsymbol{G}_n = \int_{\partial V_n} \boldsymbol{R}^T \boldsymbol{L}\,\mathrm{d}s \tag{11}$$

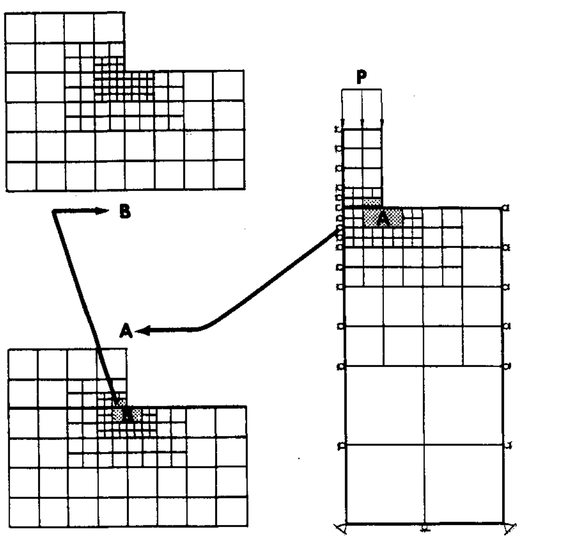

Fig. 1 Finite element mesh of the punch/contact problem.

$$\boldsymbol{Q}_n = \int_{s_{\sigma_n}} \bar{\boldsymbol{T}}^T \boldsymbol{L}\,\mathrm{d}s \tag{12}$$

$$\boldsymbol{F}_n^A = \int_{s_{c_n}^A} \boldsymbol{M}^T \boldsymbol{L}^A\,\mathrm{d}s \tag{13}$$

$$\boldsymbol{F}_n^B = \int_{s_{c_n}^B} \boldsymbol{M}^T \boldsymbol{L}^B\,\mathrm{d}s \tag{14}$$

By taking the first variation with respect to $\boldsymbol{\beta}^T$ to be zero, one obtains

$$\boldsymbol{H}_n \boldsymbol{\beta} - \boldsymbol{G}_n \boldsymbol{q}_n = 0 \tag{15}$$

Thus,

$$\boldsymbol{\beta} = \boldsymbol{H}_n \boldsymbol{G}_n \boldsymbol{q}_n \tag{16}$$

After the substitution into $\pi_{mc_n}^P$, it becomes

$$\pi_{mc_n}^P = -\tfrac{1}{2}\boldsymbol{q}_n^T \boldsymbol{G}_n^T \boldsymbol{H}_n^{-1} \boldsymbol{G}_n \boldsymbol{q}_n + \boldsymbol{q}_n^T \boldsymbol{Q}_n - \boldsymbol{q}_n^{A^T} \boldsymbol{F}_n^A \boldsymbol{t} + \boldsymbol{q}_n^{B^T} \boldsymbol{F}_n^B \boldsymbol{t} \tag{17}$$

Then for the total contact problem, the functional is

$$\pi_{mc}^P = -\tfrac{1}{2}\boldsymbol{q}^T \boldsymbol{K}\boldsymbol{q} + \boldsymbol{q}^T \boldsymbol{Q} - \boldsymbol{q}^{A^T} \boldsymbol{K}_c^A \boldsymbol{t} + \boldsymbol{q}^{B^T} \boldsymbol{K}_c^B \boldsymbol{t} \tag{18}$$

where

$$\boldsymbol{K} = \sum_n \boldsymbol{G}_n^T \boldsymbol{H}_n^{-1} \boldsymbol{G}_n = \begin{bmatrix} \boldsymbol{K}^A & 0 \\ 0 & \boldsymbol{K}^B \end{bmatrix} \tag{19}$$

$$\boldsymbol{Q} = \sum_n \boldsymbol{Q}_n = \begin{Bmatrix} \boldsymbol{Q}^A \\ \boldsymbol{Q}^B \end{Bmatrix} \tag{20}$$

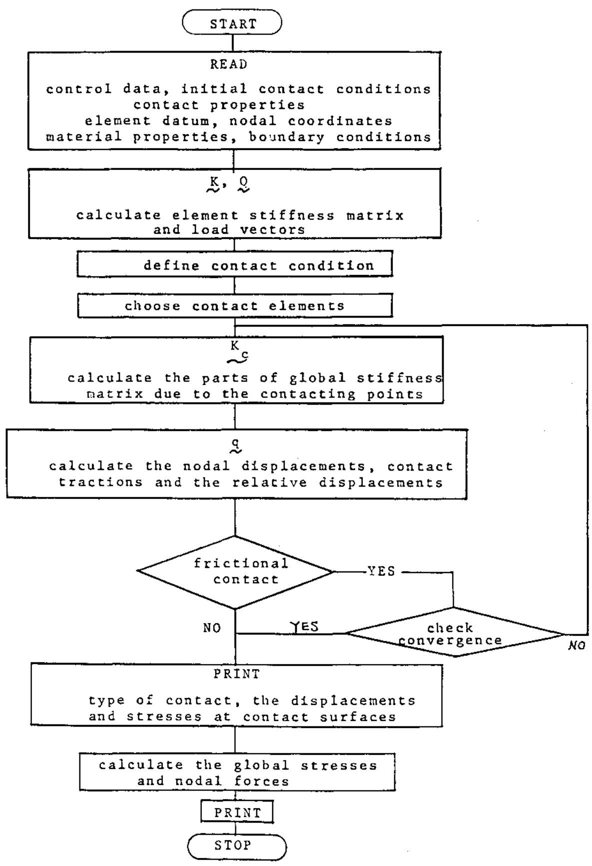

Fig. 2 Flowchart of computer program in the punch/contact problem.

$$K_c^A = \sum_n F_n^A \tag{21}$$

$$K_c^B = \sum_n F_n^B \tag{22}$$

The minimum variation of π_{mc}^P with respect to q^{A^T}, q^{B^T}, and t gives,

$$\begin{bmatrix} K^A & 0 & K_c^A \\ 0 & K^B & -K_c^B \\ K_C^{A^T} & -K_c^{B^T} & 0 \end{bmatrix} \begin{Bmatrix} q^A \\ q^B \\ t \end{Bmatrix} = \begin{Bmatrix} Q^A \\ Q^B \\ 0 \end{Bmatrix} \tag{23}$$

or

$$\begin{bmatrix} K & K_c \\ K_c^T & 0 \end{bmatrix} \begin{Bmatrix} q \\ t \end{Bmatrix} = \begin{Bmatrix} Q \\ 0 \end{Bmatrix} \tag{24}$$

where K is the structural stiffness matrix, K_c the contact node-pair matrix, q the nodal displacement vector, and Q the applied equivalent nodal force vector. In general contact problems, the size of K_c is much smaller than that of K^A and K^B.

A quadrilateral assumed stress hybrid element[8] is applied in the present analysis. This two-dimensional element can be used as either a four- or five-node element. The elastic compliance matrix of orthotropic fibrous material in plane strain is

$$C = \begin{bmatrix} \dfrac{1}{E_1} - \dfrac{\nu_{31}^2}{E_3} & -\dfrac{\nu_{21}}{E_2} - \dfrac{\nu_{31}\nu_{32}}{E_3} & 0 \\ -\dfrac{\nu_{21}}{E_2} - \dfrac{\nu_{31}\nu_{32}}{E_3} & \dfrac{1}{E_2} - \dfrac{\nu_{32}^2}{E_3} & 0 \\ 0 & 0 & \dfrac{1}{G_{12}} \end{bmatrix} \tag{25}$$

where axis-2 is the fiber direction. Thus, $E_1 = E_3$, $\nu_{32} = \nu_{12}$, $\nu_{32} = \nu_{23}$, $\nu_{31} = \nu_{13}$, $\nu_{12}E_2 = \nu_{21}E_1$.

The finite element mesh is depicted in Fig. 1, with the axis of symmetry at the center. There are 50 elements in the punch and 206 elements in the composite. The total degrees of freedom is 684. The prescribed displacements are applied at the top of the punch block and the boundaries at the sides of composite body are roller-supported.

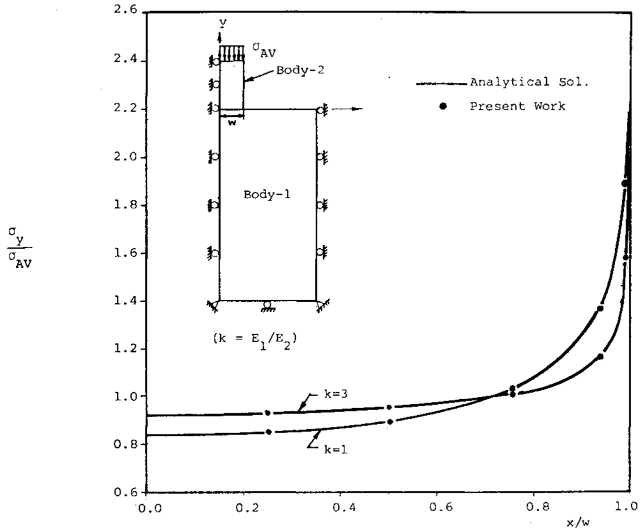

Fig. 3 Distribution of σ_y on the contacting surface; isotropic, $k = 1,3$; frictionless contact.

Table 1 Nonfrictional contact cases studied

Material of half-space plane	Material constants E_y, 10^6 psi	G, 10^6 psi	ν	Major modulus ratio k $(=E_1/E_2)^a$
	90	34.62	0.3	3.0
	30	11.54	0.3	1.0
Isotropic	18	6.92	0.3	0.6
	12	4.62	0.3	0.4
	6	2.31	0.3	0.2
	90	0.7	0.2	3.0
	30	0.7	0.2	1.0
	18	0.7	0.2	0.6
Orthotropic	12	0.7	0.2	0.4
	6	0.7	0.2	0.2
	6	0.23	0.2	0.2
	1.68	0.7	0.2	0.056
	1.68	0.065	0.2	0.056

[a] $E_2 = 30 \times 10^6$ psi, $E_1 = E_y$.

Table 2 Frictional contact cases studied

Material of half-space plane	Material constants E_y, 10^6 psi	G, 10^6 psi	ν	k $(=E_1/E_2)^a$	Coefficient of friction, μ	Slide/stick, %
	90	34.62	0.3	3.0	0.5	(0.0039/0.9961 =) 0.39
	30	11.54	0.3	1.0	0.5	(0.0039/0.9961 =) 0.39
	18	6.92	0.3	0.6	0.5	(0.0039/0.9961 =) 0.39
Isotropic	12	4.62	0.3	0.4	0.5	(0.0039/0.9961 =) 0.39
	6	2.31	0.3	0.2	0.5	(0.0039/0.9961 =) 0.39
	30	11.54	0.3	1.0	0.4	(0.01171/0.9829 =)11.91
	30	11.54	0.3	1.0	0.2	(0.375/0.625 =) 60.00
	18	6.92	0.3	0.6	0.2	(0.375/0.625 =) 60.00
	18	0.7	0.2	0.6	0.5	(0.0039/0.9961 =) 0.39
	12	0.7	0.2	0.4	0.5	(0.0039/0.9961 =) 0.39
	6	0.7	0.2	0.2	0.5	(0.0039/0.9961 =) 0.39
Orthotropic	1.68	0.7	0.2	0.056	0.5	(0.0039/0.9961 =) 0.39
	6	0.23	0.2	0.2	0.5	(0.0000/1.0000 =) 0.00
	1.68	0.065	0.2	0.056	0.5	(0.0000/1.0000 =) 0.00
	18	0.7	0.2	0.6	0.2	(0.03125/0.96875 =)3.23
	18	4.0	0.2	0.6	0.2	(0.2500/0.7500 =) 33.33
	18	7.5	0.2	0.6	0.2	(0.5000/0.5000 =) 100.00

[a] $E_2 = 30 \times 10^6$ psi, $E_1 = E_y$.

Results and Discussion

Following the formulation presented above, a finite element computer program has been developed for the two-dimensional problem. A contact surface is assumed together with the points on it. The type of contact, stick or slide, is determined by the relative movement of node pairs of the contact bodies. Thus, the variation of the contact surface and frictional effects introduce discontinuities and nonlinearities across the contact surface. A step-by-step iteration procedure is required to modify the final contact position, where both the conditions of contact and convergence are satisfied. The flowchart of the calculation consists of two loops, as shown in Fig. 2. The outer loop corresponds to a process of displacement incrementing, within which the contact condition of one nodepair varies. $\boldsymbol{K}^A$ and $\boldsymbol{K}^B$ remain constant, and the contact stiffness matrix, $\boldsymbol{K}_c$, is upgraded by using the modified Newton-Raphson elimination technique. The inner loop is to insure that the stick-slide frictional conditions are satisfied for all contact nodepairs. For the initial calculation of the first iteration, one must use an assumption made by physical inspection.

The computer program was tested for a punch/contact problem between two isotropic bodies. A good agreement has been achieved with the analytical solution[1] in the frictionless case, as shown in Fig. 3, and with the finite element solution in the frictional contact case, as reported in Refs. 5 and 7. A singular stress point near the edge of the punch is noted.

In the present work, an isotropic elastic punch is pressed against a semi-infinite orthotropic elastic body. A total of thirty cases are studied by changing the material properties of the contact bodies, which are listed in Tables 1 and 2. All the results are indicated by nondimensional terms, such as σ_y/σ_{AV} and τ_{xy}/σ_{AV}, where σ_{AV} is the average applied stress on the punch and σ_y and τ_{xy} are the normal and shear stresses, respectively. In Fig. 4 there are four curves of pressure distribution on the contact surface, representing different composite materials. It is noted that the distribution is nearly independent of the frictional conditions if the material properties remain constant, which were also seen in Refs. 5 and 7. The relative magnitudes of the pressure distribution are reversed at the local point $x/w = 0.78$. The respective states of shear stresses in the y direction on the contour of the punch are plotted in Fig. 5. For constant shear modulus, it is seen that the stiffer the material along the orthotropic axis, the lower the shear stresses. However, varying the shear moduli, as shown in Fig. 6, will give another trend; i.e., the higher the shear modulus, the higher the shear stresses.

The contact behavior on the contact surface of each case is examined and summarized in Table 2. It is clear that the

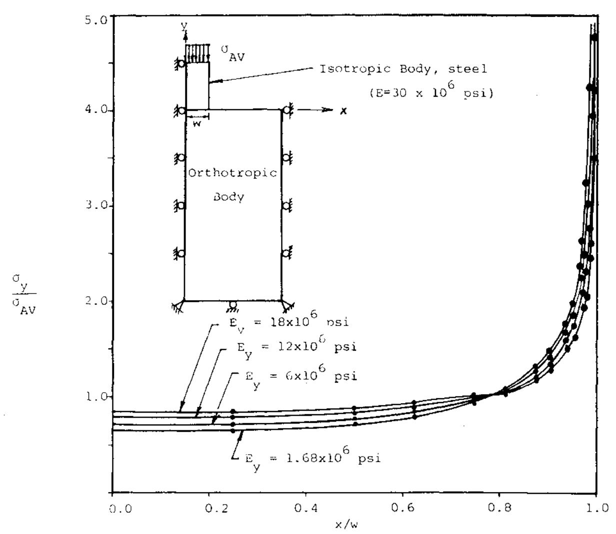

Fig. 4 Distribution of σ_y on the contacting surface, orthotropic (E_y's); frictionless and frictional contact.

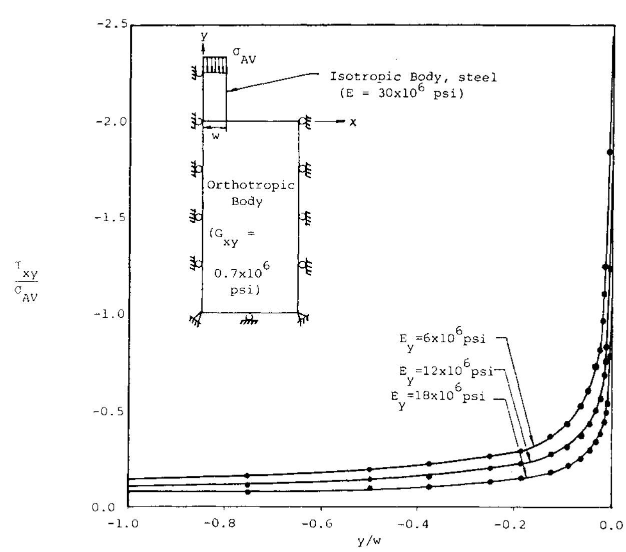

Fig. 5 Distribution of τ_{xy}/σ_{AV} along the line $x/w = 1.0$; frictional contact ($\mu = 0.2$).

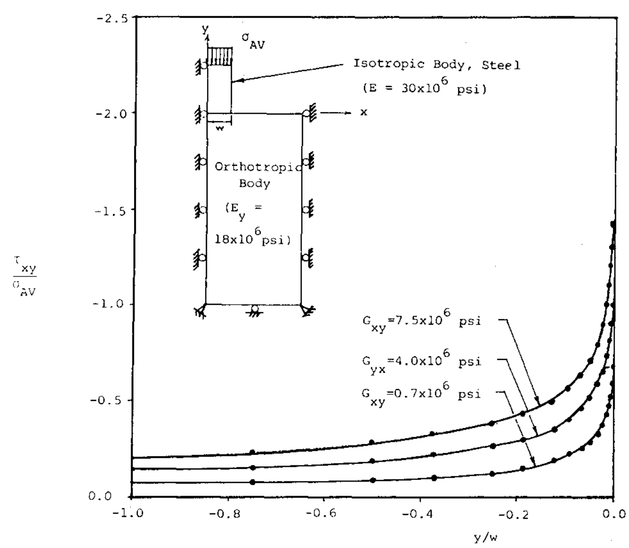

Fig. 6 Distribution of τ_{xy}/σ_{AV} along the line $x/w = 1.0$; frictional contact ($\mu = 0.5$).

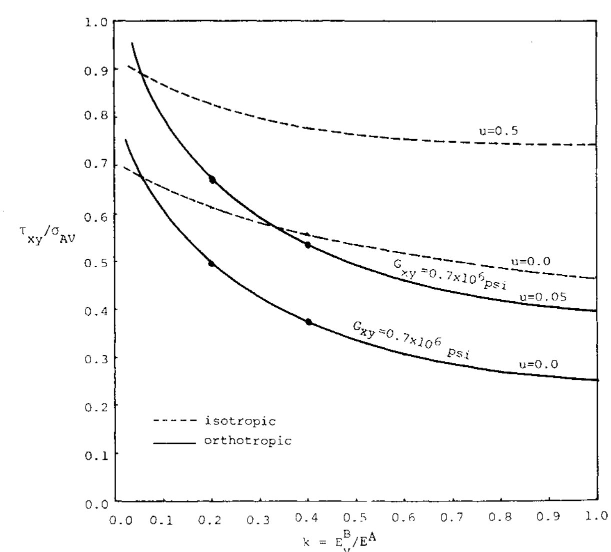

Fig. 7 Value of τ_{xy}/σ_{AV} at point $x/w = 1.0$, $y/w = -0.04687$; frictionless and frictional contact.

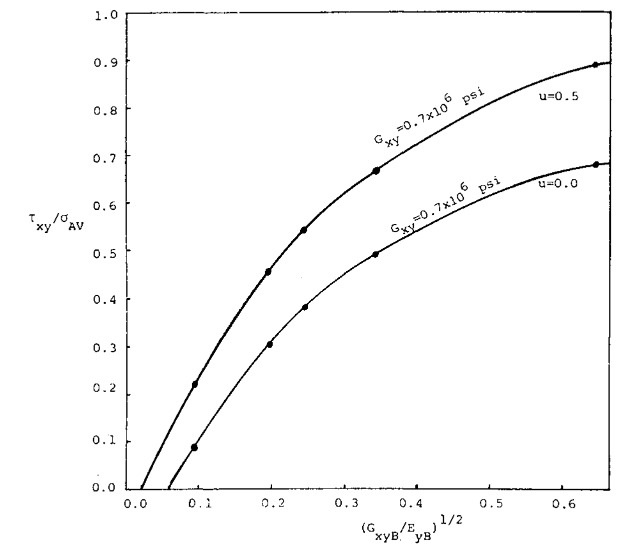

Fig. 8 Value of τ_{xy}/σ_{AV} at point $x/w = 1.0$, $y/w = -0.04687$ (y is the orthotropic axis).

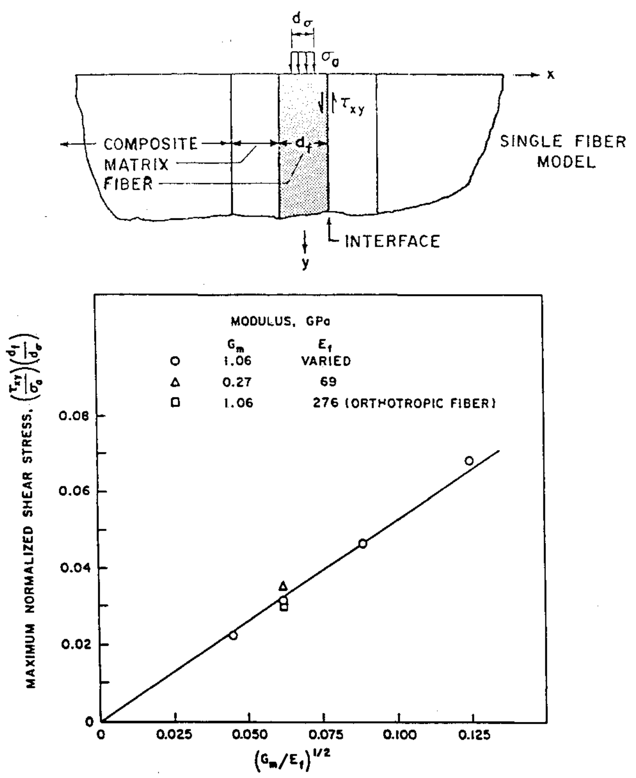

Fig. 9 Maximum shear stress at interface vs $(G_m/E_f)^{\frac{1}{2}}$ for $d_\sigma/d_f = 0.50$, imposed pressure.

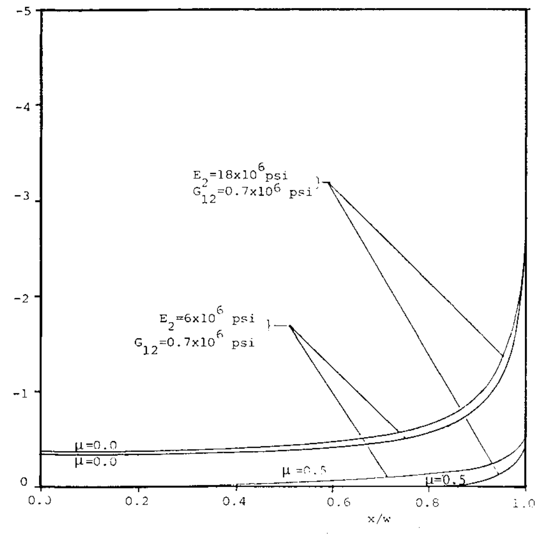

Fig. 10 Distribution of σ_x on the contact surface, orthotropic (E_y's); frictional and frictionless contact.

stick-slide phenomenon is dominated by the frictional coefficient on the surface. The relationship between the shear stresses and the relative material moduli of punch and composite are observed with respect to the factors E_y^B/E^A and $(G_{xy}^B/E_y^B)^{\frac{1}{2}}$, as shown in Figs. 7 and 8, respectively. Figure 8 indicates that the linear relationship between the maximum shear stress and $(G/E)^{\frac{1}{2}}$ observed with a single fiber model,[9] as illustrated in Fig. 9, is not observed with the punch problem. However, the trend is in a similar direction and could still be linear if the same low range of $(G/E)^{\frac{1}{2}}$ were analyzed. Figure 10 gives the distribution of transverse stress σ_x along the punch-contact region for two orthotropic materials, whose moduli in the fiber direction are 6,000 ksi and 18,000 ksi, under the frictionless and frictional conditions. It is shown that as the friction increases on the contact surface, the magnitude of stress σ_x decreases, although it is compressive in the present case.

In summary, an analysis has been presented for the punch problems with anisotropic materials. Results for typical variations in properties show that the material stiffness in the direction of loading dominates the stresses on the contacting surface with the same frictional condition. However, for the same material, varying the frictional coefficient will not affect the axial stress σ_y and shear stress τ_{xy}, but will influence the transverse stress σ_x. So, under the punch-bearing loading condition, the transverse compressive constraint to a unidirectional fiber composite will be relaxed by increasing the friction on the contacting surfaces.

Acknowledgments

The authors would like to thank Dr. Kenji Kubomura of Beloit Manhattan, Inc. for his invaluable discussion and suggestions.

References

[1] Okubo, H., "On the Two Dimensional Problem of a Semi-Infinite Elastic Body Compressed by an Elastic Plane," *Transactions of the Japan Society of Mechanical Engineering*, Vol. 18, No. 65, 1952, pp. 58-62 (in Japanese).

[2] Muskhelishvili, N.I., "Some Basic Problems of the Mathematical Theory of Elasticity," P. Noordhoff Ltd., Groningen-Holland, 1953 (translation from Russian).

[3] Galin, L.A., "Contact Problems in the Theory of Elasticity," translated by Moss, H. and Seddon, I.N.; Dept. of Mathematical Engineering Research, North Carolina State College, Raleigh, N.C., 1961 (translation from Russian).

[4] Yamada, Y., Yokouchi, Y., and Sasaoka, G., "Analysis of the Contact Problem by the Finite Element Method," *Proceedings of the 3rd Conference of the Society of Steel Construction of Japan*, 1969, pp. 412-421 (in Japanese).

[5] Ohte, H., "Analysis of Elastic Contact Stress by Using Finite Element Method," *Transactions of the Japan Society of Mechanical Engineering*, Vol. 38, No. 313, 1973, pp. 2210-2216 (in Japanese).

[6] Tsuta, T. and Yamaji, S., "Finite Element Analysis of Contact Problems," *Theory and Practice in Finite Element Structural Analysis*, University of Tokyo Press, Tokyo, Japan, 1973, pp. 177-194.

[7] Boonluator, P., "Numerical Analysis of Continua," Ph.D. Thesis, University of New South Wales, Australia, 1977.

[8] Kubomura, K. and Pian, T.H.H., "Solutions of Contact Problems by the Assumed Stress Hybrid Model," *Research in Nonlinear Structural and Solid Mechanics*, edited by McComb and Noor Compiled, NASA CP 2147, Oct. 1980, pp. 211-224.

[9] Tsiang, T.H., "Damage Development in Fiber Composites Due to Bearing," Sc.D. Thesis, Dept. of Materials Science and Engineering, Cambridge, Mass., Feb. 1983.